Simulation of a lattice model for the evolution of Si(001) surfaces exposed to oxygen at elevated temperatures

C. Ebner, J. V. Seiple, and J. P. Pelz
Department of Physics, The Ohio State University, Columbus, Ohio 43210
(Received 19 April 1995; revised manuscript received 17 July 1995)

A lattice model for the evolution of silicon (001) surfaces reacting with an oxygen atmosphere is presented along with results from simulations of the model. Numerous features of experiments are reproduced such as the simultaneous production of pinning centers and of Si etching, leading to long fingers on terraces terminated by oxide islands. Particular study is made of the rate of oxide-island production as a function of oxygen dose, temperature, and the rate of oxygen deposition. The results show the same general trends as scanning tunneling microscopy experiments and simple rate equations in the initial stages of the process but differ significantly in the later stages where the experiments show saturation of the island density while the model does not. From comparison of the simulations and experiments, inferences are drawn concerning the mechanisms which control the nucleation of stable oxide islands.

I. INTRODUCTION

The behavior of silicon surfaces under conditions of growth, as in molecular-beam epitaxy with Si or Ge atoms,[1–7] or etching, as in bombardment with Xe or Ar ions,[8–12] has been the topic of considerable research in recent years. A related phenomenon, the behavior of Si surfaces reacting with oxygen, has also been researched extensively,[13,14] especially quite recently.[15–23] Detailed information at the atomic level can be obtained using a variety of techniques, most notably scanning tunneling microscopy (STM). Theoretical work has typically been of two kinds, either microscopic calculations[24–27] of the structure of adsorbed species, surface defects, etc., or simulations of models[28–32] of adsorption, diffusion, and desorption in which the parameters are chosen phenomenologically and/or with input from microscopic calculations. The first approach allows treatment of only a relatively small number of atoms; one learns a great deal about localized configurations but not much about large-scale structures. The second allows study of large-scale structures but suffers from considerable oversimplification so that no single model can be expected to reproduce all observed features or to have reliable quantitative predictive capabilities for a broad range of phenomena.

In this paper we describe simulations of a model of adsorption, diffusion, and desorption on a silicon (001) surface. Like all such models it contains numerous parameters, the choice of which has been guided by experimental results, microscopic calculations, and others' work on similar models. The motivation for constructing the model was to reproduce at least qualitatively the results of recent experiments by Seiple and Pelz,[21] in which vicinal Si(001) surfaces at elevated temperatures are exposed to low-pressure, gaseous molecular oxygen, resulting in simultaneous etching of the surface (one to three layers of silicon atoms removed) and buildup of oxide islands, which act as pinning sites.

In that study a model was proposed to explain the initial pressure and temperature dependence of the measured oxide-cluster nucleation rate.[21] The basic premise was that O_2 adsorbs onto the surface, dissociating into mobile oxide "monomers." A diffusing monomer either desorbs from the surface (causing etching), joins with another diffusing monomer to nucleate a two-cluster, or attaches to an existing stable cluster causing growth. For simplicity it was assumed that the two-cluster was stable, and could not diffuse, desorb, or break apart. In the present study, this model will serve as the basis for oxygen behavior and will be supplemented with the behavior of the underlying silicon lattice as explained in Sec. II.

In addition to explaining the observed oxidation behavior, we want the model, with the same parameters, to reproduce qualitatively both the observed epitaxial growth behavior of a silicon (001) surface and the etching behavior observed when silicon is bombarded by, e.g., rare-gas ions. Although the data are not presented here, simulations of these phenomena do qualitatively reproduce the experimental results as explained briefly in the summary.

Finally, following more recent experimental studies[22] of oxidation of Si(001) surfaces in which considerably more than three layers of Si are removed, we have done extensive simulations of a simpler model in order to examine the rate at which oxide islands are produced as a function of temperature, oxygen pressure, and dose. Results from these simulations are compared with the experiments and also with an analysis of a set of appropriate rate equations.

The remainder of the paper is organized as follows: Section II presents the model and choices of parameters, while Sec. III gives a brief description of the STM experiments in which many layers of silicon are removed by oxygen adsorption and desorption with the concomitant production of oxide islands. Results are presented in Sec. IV, and Sec. V is a summary.

0163-1829/95/52(23)/16651(14)/$06.00

II. MODEL

The model we have simulated is based closely on that of Barnett and Rockett.[28] It is a solid-on-solid model for a diamond structure. The silicon crystal is represented by a square array of cells of edge length $a_0 = 3.84$ Å, the unit translation of the Si diamond structure. Within each cell (i,j) there is a helical column of atoms of height $h(i,j)$ with no vacancies in the column. Atoms in a column are arranged in a spiral pattern with a period of 4 in such a way as to reproduce the diamond structure of silicon. In particular, any atom in the bulk solid has two nearest neighbors in the layer immediately below it and two more in the next-higher layer. Surface dimers are incorporated into the model by allowing a surface atom with no nearest neighbors above it to be in any of three states labeled by $k = -1, 0, +1$. In state $k = 0$ the atom is imagined to be at the site of the diamond structure. In the other two states it is displaced to one side or the other in the direction of a next-nearest-neighbor site in the same layer, perpendicular to the direction of the bonds to the nearest neighbors in the next-lower layer. When an atom forms a dimer with one of these neighbors, its state becomes $k = +1$ or $k = -1$, depending on which neighbor is chosen, while the state of its partner is $k = -1$ or $k = 1$, respectively. The model does not allow for buckled dimers, nor does it allow surface dimers in which one of the member atoms has a bond to an atom in a higher layer.

Simulations proceed by allowing atoms that have no bonds to atoms in higher layers to diffuse on the surface. That is done by picking at random one of the four $\langle 110 \rangle$ directions in the plane of the surface and determining whether the next-nearest-neighbor site in the same layer in that direction is available. If the site is empty but not available because one of the nearest-neighbor sites in the layer below is not occupied, then a move to the latter site is considered. It, too, may not be available, in which case the attempted move is abandoned. If both underlying sites are available, one is picked at random and a move attempted to that site. A final possibility is that the next-nearest-neighbor site to which the move is attempted is already occupied, in which case we test for a possible move to a higher nearest-neighbor site of the occupied one. That is done in the same way as for moves to the next-lower layer. If an acceptable move is identified, there is still the question of acceptance. That is decided using standard Monte Carlo procedures and is discussed below when we introduce the activation energies for the moves.

Our model differs from that of Ref. 28 in that we permit the motion of a surface dimer as a unit. The allowed moves are more restrictive than for single atoms. Only moves in the same layer by a single lattice spacing in the direction perpendicular to the surface dimer bond are allowed. This move is included because several experiments[33,34] provide evidence that it is an important one for the motion of steps. More precisely, the experiments show that typically a pair of dimers will move, if not precisely together, then in a short time. The reason apparently is that if just one dimer at a terrace edge is displaced perpendicular to the step, that will result in a relatively high energy configuration because of the net loss of surface bonds in the layer below, encouraging either the first dimer to return to its original position or a second one, initially behind the first, to follow the first. Although we allow just one dimer at a time to move in our simulations, we take into account (see below) the change in energy in the surface bonds and in fact find in the simulations that the lengths of dimer rows at the edges of B terraces tend to change by multiples of two, which means that a second dimer follows the first with some alacrity.

In simulations of epitaxial growth, atoms are added to random sites periodically during the simulation, $h(i,j) \rightarrow h(i,j) + 1$, with the condition that no overhang be produced in the process. If the randomly chosen site does not meet this criterion, neighboring sites are examined until one is found which does, and the adatom is placed at that site. Etching with no impurity buildup is simulated by removing atoms from random sites periodically, $h(i,j) \rightarrow h(i,j) - 1$, with the condition that no overhang be produced.

In the case of reaction with oxygen, the production of oxide is put into the model by specifying that when a Si atom is removed, meaning when $h(i,j)$ is reduced by unity, the Si atom is incorporated into a SiO complex at that site on the surface. This complex can diffuse and desorb and can also meet other SiO complexes and become part of an inert oxide cluster or island. Also, when there is a SiO complex at site (i,j), then $h(i,j)$ is not allowed to change; neither are the heights at the four neighboring lattice sites. Hence the SiO pins underlying silicon, and the pinning site is permanent if there is an oxide cluster.

The final type of move included in our simulations, as in Barnett and Rockett's,[28] is the "bond flip," in which a surface atom in state $k = 0$ can form a surface dimer with a next-nearest neighbor that is already participating in a surface dimer. These moves enable antiphase boundaries to be removed and produced.[28]

Following any move of a Si atom, the surface will relax. If the atom that moves was part of a surface dimer, the former partner will be free to form another dimer. Also, when an atom leaves a site, either of the two underlying nearest neighbors may be free to form a dimer. If an atom moves to a site where one or both of the underlying atoms is in a surface dimer, then the dimer(s) must be broken. As a consequence the partner atom or atoms are free to form new dimers. Similarly, the atom that has been moved may be able to form a dimer. In the simulations, all possible new surface dimers are formed as part of a move.

There are numerous parameters in the model specifying the attempt rates and energy barriers. All simulations reported here employed one set of parameters, which are given in Table I. In the interest of simplicity, and in the spirit of a model which, although quite complex, is certainly much less complex than the actual system, we set many parameters equal in the absence of evidence that would dictate otherwise. This sacrifices

TABLE I. Activation energies for possible actions in the simulations. All actions used an attempt frequency of 1×10^{12} $\sec^{-1}$ except for monoxide desorption ($\nu_{ce} = 4 \times 10^{19}$ $\sec^{-1}$, from Ref. 35) and for monoxide diffusion ($\nu_{cd} = 1 \times 10^{16}$ $\sec^{-1}$). See the text for a physical description of each barrier and references to values chosen.

adatom diffusion	height change	dimer bond breaking	second-nearest neighbor		dimer diffusion	monoxide diffusion	monoxide desorption	oxide nucleation
ϵ_d	ϵ_s	ϵ_b	ϵ_o	ϵ_m	ϵ_p	ϵ_{cd}	ϵ_{ce}	ϵ_{ci}
0.65	0.65	0.70	0.15	0.075	1.30	2.40	3.40	0.43

flexibility and the possibility of better quantitative agreement with experiment, but at this stage of our studies we feel that simplicity is the greater virtue.

First, an isolated adatom has a barrier against diffusive motion on a terrace in the absence of any other complicating factors such as nearby steps or next-nearest neighbors on the same level. The diffusion is known to be highly anisotropic, and the barriers for motion parallel to a row of underlying dimers and motion parallel to such a row may well be different. We nevertheless introduce the same barrier of height ϵ_d for both of these possible motions. In order to make the diffusion anisotropic, we reject moves that result in a net decrease of the number of surface dimers. This procedure is explained below in greater detail.

There is likely an additional barrier to motion up or down a step, and that barrier may depend on whether it is an A- or B-type step as well as whether the atom moves up or down. In the absence of any detailed information about the relative barriers for these moves, we have a single barrier height ϵ_s, in addition to the barrier ϵ_d, for all moves over a step. We have, for no physically motivated reason, set $\epsilon_s = \epsilon_d$. That is, qualitatively speaking, the model behaves reasonably with this choice so we have no good reason for making a different one.

A move or change of state by an atom that is initially in a surface dimer will have an additional barrier for motion because the dimer must be broken. We associate an energy ϵ_b with the breaking of the dimer bond.

In order that the 2×1 structure be favored over other possible configurations of the reconstructed surface, we introduce k-dependent second-nearest-neighbor interactions within a layer. Two such neighbors in the same state share an energy $-\epsilon_o$; two in different states share an energy $-\epsilon_m$; and ϵ_o and ϵ_m are positive. The difference between them comes into play if one changes the states of the atoms without displacing either one; by choosing $\epsilon_m < \epsilon_o$, we cause the 2×1 reconstruction to be favored. Finally, ϵ_m is set equal to one-half of ϵ_o more as a matter of simplicity than anything else.

For motion of an isolated dimer pair, we introduce an activation energy ϵ_p. If the members of the pair have second-nearest neighbors in the layer, the activation energy is increased according to the prescription set forth in the preceding paragraph. Moreover, we set $\epsilon_p = 2\epsilon_d$.

Finally, we need to attempt frequencies for these moves. The attempt frequencies for the motion of a single atom, for motion of a dimer pair, and for bond flips are all equal and designated as ν.

The addition or removal, in the case of no oxide buildup, of Si atoms proceeds by adding or removing an atom at a randomly chosen cell at fixed time intervals τ. If τ_l is the time for a single layer to be added or removed, then $\tau = \tau_l / N_c$, where N_c is the number of cells in the system. In simulations of the reaction with oxygen, O atoms are assumed to be added on the surface at randomly selected cells at time intervals τ. These remove locally a Si atom to form a SiO complex at that cell, which can then diffuse with an energy barrier ϵ_{cd} and attempt frequency ν_{cd} as well as desorb with an energy barrier ϵ_{ce} and attempt frequency ν_{ce}. To maintain simplicity the diffusion is isotropic and independent of the underlying surface structure. We introduce an additional barrier ϵ_{ci} for a diffusive move that brings a SiO complex to a site in the nearest-neighbor cell to another SiO complex. This energy is a barrier to the nucleation of an oxide cluster, which involves changes in the bonds within the SiO complexes. Once a SiO dimer is formed, it is assumed to be stable against further diffusion or desorption, although additional SiO complexes can attach to it, also with the nucleation barrier ϵ_{ci}. A SiO complex acts as a pinning site for Si atoms because no Si atom in the same cell or a nearest-neighbor cell is allowed to leave. Neither is a Si atom allowed to move into such a cell.

The configuration of the system at the start of a simulation has four terraces with parallel straight edges, the highest terrace being at the top of the figures displayed in the following section. Periodic boundary conditions are applied in the x or horizontal direction, while, in the y direction, an atom that moves out of the system across the bottom boundary reappears at the top (four layers higher), and one that moves out by crossing the top boundary reappears at the bottom. The system is 96×95 cells in size; each terrace has a width of either 24 or 23 cells. Systems with fewer terraces and different sizes have been simulated to a lesser extent to explore size dependences.

The simulations proceed in a standard fashion. For the diffusion of a Si atom, a cell is selected at random and an attempt made to move the uppermost atom in that cell. The attempt is accepted with a probability based on the barrier for the particular move. In order to make the simulations computationally tractable in general, especially in the study of extensive etching, some shortcuts must be employed. First, rather than accepting a move with probability $\exp(-\beta E)$, where E is the energy barrier and β is the inverse temperature, we scale all probabilities by

a factor $f > 1$; in effect, the mean time elapsing between attempted moves at a given site is not the inverse of the attempt rate, or $1/\nu$, but is rather f/ν. In this way the simulation is sped up by a factor of f while maintaining the mean number of moves of any given type in a given amount of "real" time. The factor f is typically chosen so that there are 1000 attempted moves per surface atom between the deposition of individual atoms (oxygen or silicon), and that makes it possible to simulate the deposition or removal of several atomic layers at relatively high temperatures at rates on the order of 500 sec per layer. Typically, one day of CPU time is required to simulate the addition or removal of one layer using a VAXstation 4000-90.

Unfortunately, the scaling factor f is usually so large that the probability of accepting the most common moves, e.g., the diffusion of a lone atom on a flat terrace, can become much larger than unity, of order 1000 to 10 000. Our response is simply to accept any attempted move of this kind. The result is that our procedure underestimates the distance the adatom will diffuse on a flat terrace in a given amount of time by a quite large factor, up to 100. We believe that this shortcoming is not of great importance, because even under these conditions adatoms still can sample quite effectively the structures on the relatively narrow terraces in our systems. That is, they still diffuse a distance on the order of 30 cell lengths, more than 100 Å, between addition of a single Si or O to the entire surface. The important moves for determining the morphology of the surface, which involve moves up and down steps and the breaking of surface bonds, are sufficiently rare, or unlikely, that even after scaling the probabilities of these moves by the factor f they are still considerably smaller than unity and so are treated correctly in the mean. We have tested the consequences of rescaling the attempt frequencies by making a number of runs in which the rescaling is either not done or is done by different factors, comparing such essential results as the rate of oxide-island formation for different scaling factors. For all cases tested the results are independent of the rescaling, to within statistical uncertainties.

Another consequence of this rescaling of the attempt frequencies is that the scaled probability of accepting a bond-flip move is often larger than unity. In this case we simply reduce the probabilities of accepting all bond-flip moves by a constant factor so that the relative probability of different bond flips is given correctly. The only consequence of these moves is to allow antiphase boundaries to be annealed out (or produced), and although we have not treated correctly the rate at which that happens, the consequences are not of great import for the behavior of this model, at least for the phenomena reported in this paper.

A second approximation that increases the speed of the simulation is not to attempt moves in which a single atom with four next-nearest in-plane neighbors is removed and elevated to the next-higher layer. We catalog cells according to how many in-plane second neighbors the topmost atom has and so construct a list of cells containing movable atoms and select the atom to be moved from this list. The list must be updated continually. Nevertheless, there is a significant improvement in speed because most surface atoms have four in-plane second neighbors. The disadvantage is that there is no spontaneous creation of vacancies in a terrace by ejection of an atom, an event which is in any case rare except at very high temperatures.

Finally, one should take into consideration some properties of the state that result from a move. If the energy of the final state lies higher than the top of the barrier that must be crossed for the atom to escape from its initial position, then that presents a further impediment to the move. The most obvious way this can occur is if surface dimers are broken in addition to any in which the moving atom was initially involved. For example, if an isolated adatom moves in a direction parallel to the underlying surface bonds on the reconstructed 2×1 surface, there can result the net loss of one surface bond after the surface reconstructs following the move.[29] That will likely, depending on the relative size of various energy parameters, give a final state which is, relative to the initial one, higher in energy than the barrier for migration. In principle, one should determine for each move whether that is the case and adjust the probability of accepting the move accordingly. That, however, necessitates a considerably more complicated code that tests not only for the energy barrier to any given move but also determines the energy of the final state before deciding whether to accept or reject any move. We have written such a code, but it runs so slowly on the available computers as to be useless for simulations on the scale of interest to us. A simpler approximate procedure that we have adopted is to reject any move by a single atom that results in a net loss of surface bonds aside from a bond in which the moving atom may have been initially involved (and which is taken into account in the activation energy for the move). In the case of dimer or atom-pair motion, which has a relatively high energy barrier, we reject moves that result in the net loss of more than one surface bond. This procedure guarantees, in particular, that single-atom diffusion across dimer rows in the underlying surface will be much less prevalent than diffusion along rows, because motion across underlying dimer rows requires, when the atom attempts to move into the "trough" between two dimer rows, the breaking of one surface bond while not allowing any new surface bonds to form. This suppression of diffusion across dimer rows produces highly anisotropic diffusion of an isolated atom, consistent with experimental findings.[7]

The activation energies are determined in part from prior experiments and in part from numerous preliminary simulations with different sets of parameters, in which we sought to obtain behavior with a qualitative resemblance to experimental results. The set that has been used exclusively in this work is displayed in Table I. Energies are in eV. The attempt frequencies ν, ν_{cd}, and ν_{ce} are noted in the caption.

The energies $\epsilon_d = 0.65$ eV and $\epsilon_b = 0.70$ eV are typical of those that emerge from experimental studies; $\epsilon_o = 0.15$ eV and $\epsilon_m = 0.075$ eV are such that the energy per atom of an S_B step is 0.15 eV while that of an S_A step is 0.075 eV, numbers in the general range indicated by experi-

ment and theory and generally in line with what have been used by others in similar simulations.[28–30] The barrier for pair diffusion is set equal to twice the barrier for single atom diffusion. When that energy is added to the energy required to escape from any next-nearest neighbors in the plane (ϵ_o or ϵ_m), the net is in the range suggested by experiments,[34] 1.4 to 1.7 eV. As for the barrier to moving up or down a step, that is somewhat controversial, some experiments providing evidence that there is no significant barrier at least to downward moves over S_B steps[7] while others suggest fairly formidable barriers to interlayer hopping.[9] Experiments suggest the values for the barrier associated with SiO desorption[35,36] (ϵ_{ce} = 3.0–3.4 eV) and also the total barrier against growth of oxide islands[21,23] (3.3–4.0 eV). The latter is extracted from the temperature dependence of the oxide-cluster density and should be a function of the desorption energy (ϵ_{ce}), diffusion energy (ϵ_{cd}), and an additional nucleation energy (ϵ_{ci}). Starting with the model of Ref. 21, the total barrier to oxide nucleation should be $2\epsilon_{ce} - \epsilon_{cd} - \epsilon_{ci}$, which implies $\epsilon_{cd}+\epsilon_{ci}$ should be in the range 2.0–3.5 eV.

Attempt rates are proverbially difficult to determine with precision; the choice we have made of $\nu = 10^{12}$ $\sec^{-1}$ is typical.[28] The attempt rate for desorption of a SiO, $\nu_{ce} = 4\times10^{19}$ $\sec^{-1}$ is at the upper end of the range inferred from experiments,[35] although it is very large in comparison with values typically employed in models of this kind. Finally, the attempt rate for SiO diffusion, $\nu = 10^{16}$ $\sec^{-1}$, was chosen in order that the model produce an appropriate, in comparison with experiments, balance between oxide-cluster formation and oxide desorption.

The CPU time required by a VAXstation 4000-90 to remove or add a single layer of Si atoms in a 95 × 96-cell system is about 20 h, making it rather impractical either to simulate larger systems or to run long enough to remove or add more than a few layers. For this reason, we have also simulated a drastically simplified model that is intended to study only the appearance and growth of oxide islands and that ignores completely the structure of the underlying Si crystal. This model is the same as the one just described insofar as the behavior of SiO complexes is concerned. That is, they are introduced periodically and can diffuse, join other SiO clusters, or desorb, and that is all there is to it except for the following: In addition to doing simulations in which a cluster of two SiO complexes is inert, as in the basic model, we do simulations in which a cluster of three SiO complexes is required to form an inert object. For a cluster of 2 we consider two possibilities: first, that either of the SiO's can desorb with the same probability as an isolated SiO; and, second, that either SiO can desorb with a probability that is reduced by the factor $\exp(-\epsilon_{ci}/kT)$ relative to that for an isolated SiO. Either way, the rate of production of stable clusters will be significantly reduced by the fact that a cluster of two is not stable. Notice that we do not include moves in which a binary cluster dissociates without one member of the pair desorbing. That can easily be done but is not essential if one merely wants to explore the consequences of unstable binary clusters. We have been able to simulate much larger systems (up to 1000^2 cells) for much longer times using this simplified model, making it possible to compare directly with experiments in which many layers of Si are removed by oxidation-induced etching.

III. EXPERIMENTS

The experimental procedures have been discussed elsewhere.[19,21] In brief, Si(001) samples were cleaned by resistive heating *in situ* to 1250 °C. The temperature was then lowered to 900 °C at which point an O_2 pressure of 6×10^{-8} torr was introduced to the chamber to etch the first couple of layers of Si. To begin oxide nucleation the temperature was simply lowered to the desired range without interrupting the flow of O_2. This drop in temperature causes the oxidation conditions to cross over from the strictly oxidation-induced etching regime into a regime in which both etching and oxide-cluster nucleation occur simultaneously.[22] Via this method the surface was purged of residual surface contaminants from the flash and the O_2 pressure could be stabilized before starting the oxide-cluster nucleation. Occasionally, as a check, the process was interrupted after the 900 °C etch and STM scans verified that the surface was in fact *free* of pinning sites. After the desired dose, the O_2 was turned off and the sample was quenched to room temperature and scanned. The oxide-related nucleation centers prevented the surrounding Si from etching, thereby creating islands with characteristic defects. These *pinned* islands could then be easily counted, providing a measure of the number of oxide-related clusters on the surface.

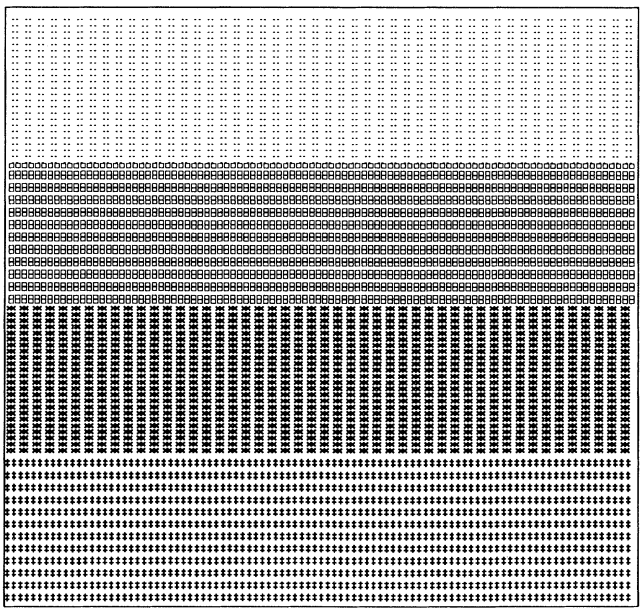

FIG. 1. The initial surface with four terraces, the highest being at the top of the figure. Individual atoms on each of the four terraces are represented by dots (·), squares (□), multiplication symbols (×), and pluses (+).

IV. RESULTS

The results presented in this section are for the etching of a silicon (001) face by interaction with molecular oxygen and subsequent desorption of SiO complexes, which occurs simultaneously with the formation of oxide clusters on the surface. The starting configuration is shown in Fig. 1. The top atom in each cell is represented by a symbol that depends on the height. On the top terrace, the symbol is a dot. Atoms on the next three terraces, moving downward, are represented by a square (□), a "times" (×), and a "plus" (+). Open circles (there are none in Fig. 1) represent SiO complexes. The terrace below the one at the bottom is equivalent to the topmost terrace and an atom at this height is represented once again by a dot. When a symbol represents an atom in a surface dimer, it is displaced slightly so that the symbols for the atoms in a particular dimer are relatively close to one another.

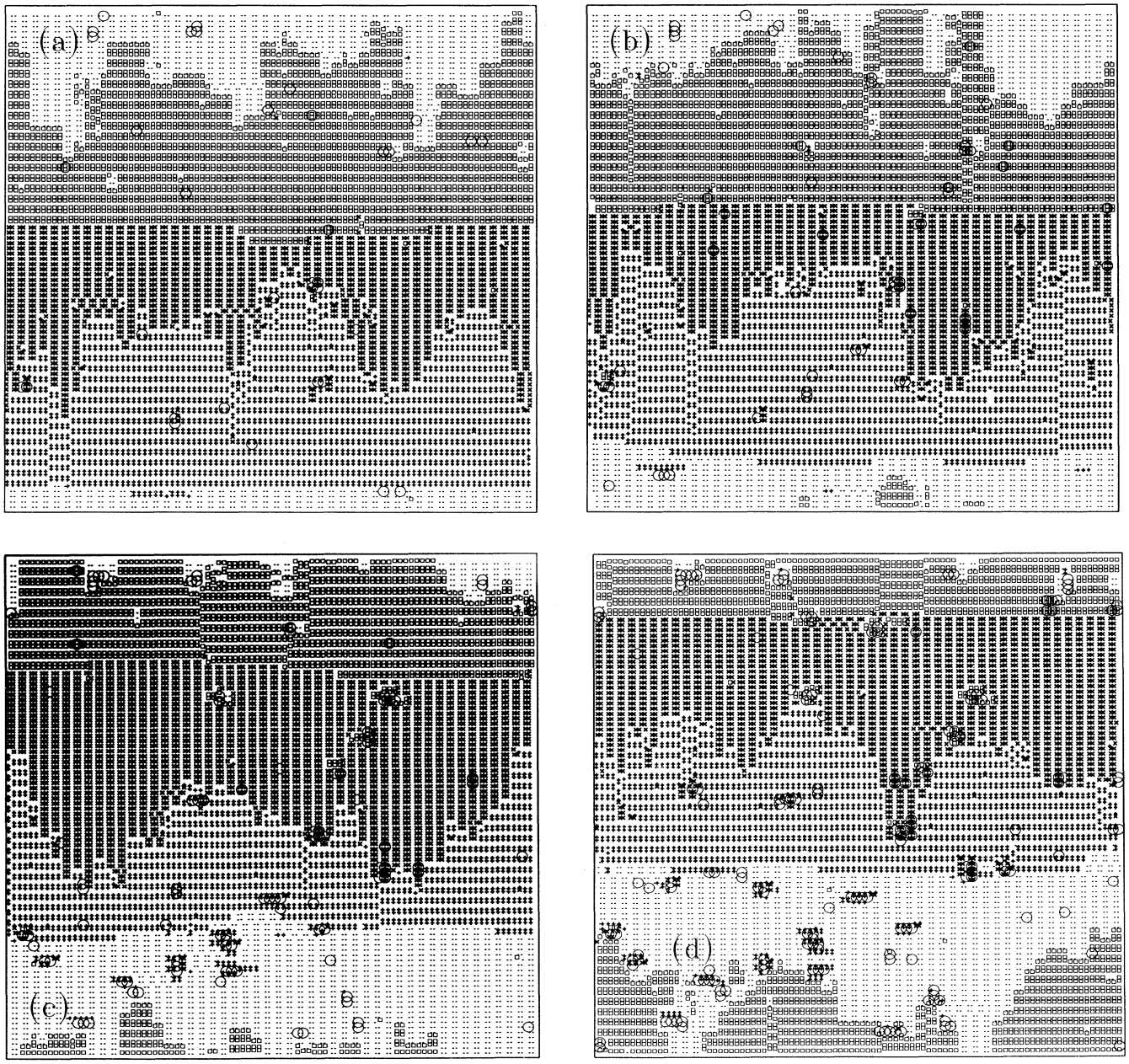

FIG. 2. Surfaces at 600 °C after (a) 0.3, (b) 0.5, (c) 1.0, (d) 1.5, (e) 2.0, and (f) 3.0 ML of Si have been removed through reaction with oxygen; $\tau_l = 500$ sec. The large open circles represent SiO complexes; other symbols are as in Fig. 1.

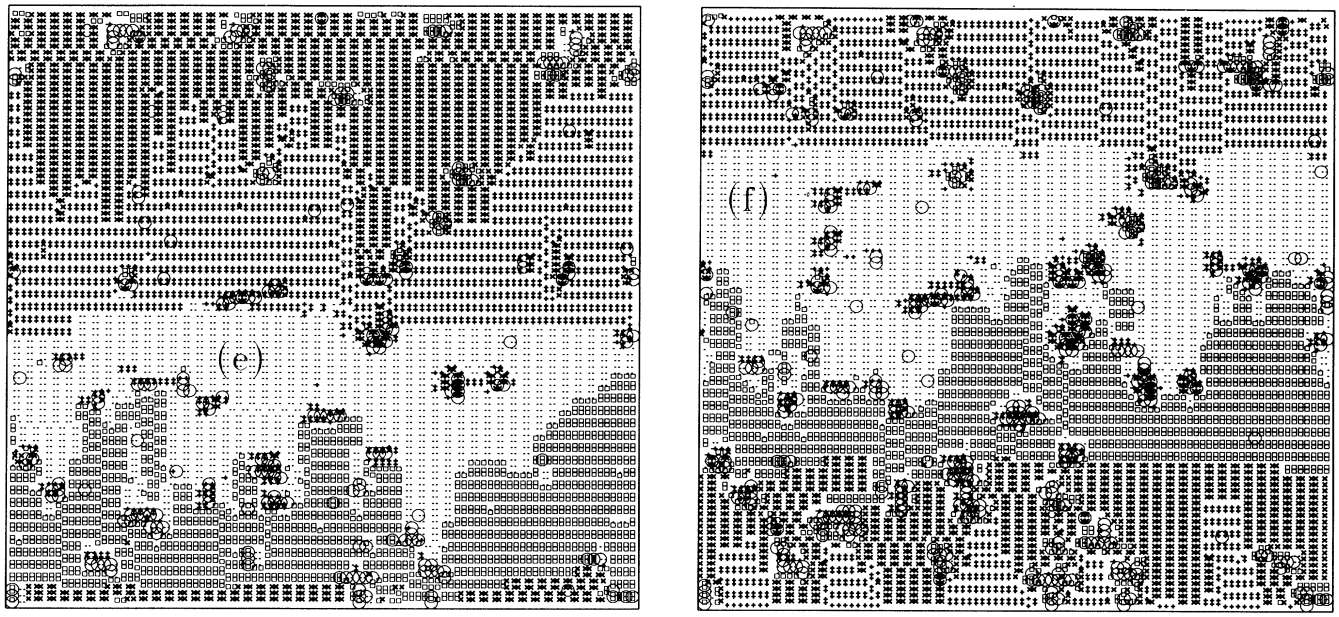

FIG. 2 *(Continued).*

Simulations have been done for temperatures in the range 590–650 °C and for τ_l from 250 to 1500 sec. They are long enough to remove three or more layers of silicon from the surface. Typical examples of the surface structure as a function of the amount of material removed are shown in Fig. 2, which is for $T = 600\,^{\circ}\mathrm{C}$ and $\tau_l = 500$ sec after (a) 0.3, (b) 0.5, (c) 1.0, (d) 1.5, (e) 2.0, and (f) 3.0 ML of Si have been removed. Once an oxide cluster forms, the silicon immediately around that cluster can no longer be etched away and so an island is formed which, relatively speaking, rises higher above the surrounding region as Si continues to be removed from the latter. Also, because material tends to be removed by retraction of individual dimer rows ending in S_B steps, these pinning sites can result in relatively long fingers of B terrace, pinned at the end, sticking out above the next-lower A terrace as material in dimer rows on either side of the pinning site is eaten away. Eventually, such fingers are eaten through from the sides, leaving just an outcropping of Si immediately around and under the oxide island. An example may be seen in Figs. 2(d) and 2(e). In roughly the middle of the former there is a relatively long finger on the B terrace, represented by $\times$ symbols, pinned at its end and in its middle by oxide clusters. By the time of Fig. 2(e), this finger has been broken between the oxide clusters. Similar behavior is seen in experiments,[21,22] although in general the lengths of the fingers formed in the simulations are not as large as what is seen in experiments. However, longer fingers can be obtained with small changes in the model's parameters, suggesting that more quantitative agreement with experiment is possible.

If the time τ_l is increased, corresponding to lowering the oxygen pressure, then a SiO complex will have a greater liklihood of desorbing as opposed to finding another complex or cluster. Hence the rate at which pinning centers form is reduced. We have done simulations with a range of τ_l. The surfaces generated in this manner have much the same appearance as those shown in Fig. 2, and from them we are able to determine the rate of oxide-cluster formation and its dependence on τ_l. However, there is some question, as to precisely how to make comparison with experiments. From the experiments one typically determines the density of oxide clusters of a certain size or outcroppings of a certain height. The resolution of the measurements is often such that the mere joining of two SiO species is not enough to register as an oxide island. Rather there is some larger minimum size of clusters necessary for detection. In the simulations, on the contrary, one may easily count the number of oxide clusters of any size. Another reason why there will be some ambiguity about a comparison is that two distinct, but sufficiently nearby, oxide clusters may be seen in an experiment as a single island or pinning site whereas in the simulation they can be identified as separate defects.

The simplest analysis of the simulations is to count the number of oxide clusters of size greater than one. We show in Fig. 3 the number of clusters as a function of the number of layers removed as found from simulations at 600 °C with τ_l between 250 and 1500 sec. In each case the number of clusters increases approximately linearly with time until the cluster density becomes large enough to suppress the nucleation rate, because newly formed mobile SiO complexes are more likely to run into existing clusters than to meet single SiO complexes. At longer times, the number of clusters reaches a maximum and eventually decreases because growing clusters merge with neighboring ones. The simulations demonstrate that the

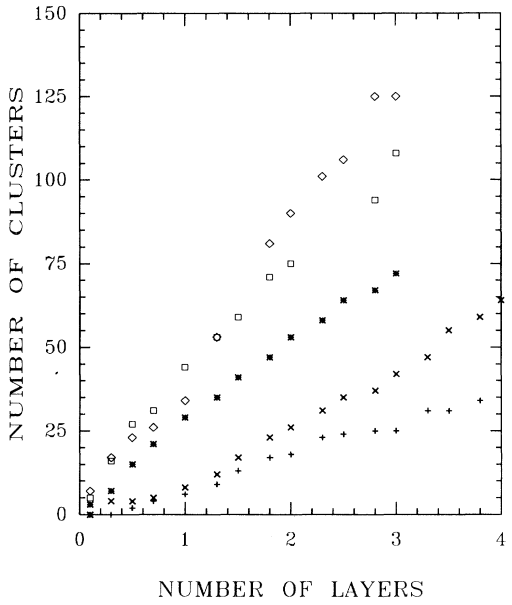

FIG. 3. The number of oxide clusters, defined as aggregates of two or more SiO complexes, is shown as a function of time at $T = 600\,^{\circ}\mathrm{C}$ for τ_l equal to 1500 (+), 1000 (×), 500 (*), 375 (□), and 250 (◇) seconds. The system is of size 95 × 96 cells.

maximum cluster density depends on the rate at which layers are etched away, i.e., on the pressure of the oxygen, being smaller when the rate of etching is smaller.

From the regime of linear growth, we have extracted the growth rate of the cluster number per unit area J_p. Figure 4 is a log-log plot of J_p as a function of $1000/\tau_l$.

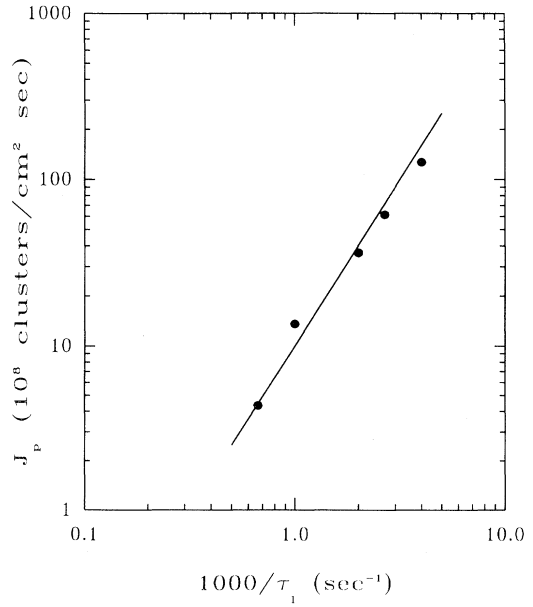

FIG. 4. The pinning center nucleation rate J_p, in units of $10^8/(\mathrm{cm}^2\,\mathrm{sec})$ is shown vs $(1000/\tau_l)$ sec^{-1}. A line of slope two is included for reference.

Also shown is a straight line of slope 2. The points fit such a line quite well, which is not surprising since a pinning center is formed in this model by the meeting of two SiO complexes. Moreover, given that[21] a τ_l of 250 sec corresponds to an oxygen pressure of about 10^{-7} torr, assuming a sticking coefficient of 0.04 for an oxygen molecule striking the silicon surface, Fig. 4 may be directly compared with Fig. 3 of Ref. 21. The two differ in that the rate at which pinning sites appear in STM images is approximately proportional to the oxygen pressure to the 2.4 power. Moreover, the magnitude of J_p from the simulations is some 100 times larger than what is extracted from the experiments.

It is not difficult to think of a number of reasons for the disparity between the rates at which clusters appear in the experiments and in the simulations. For one, the rate at which clusters are formed is strongly temperature dependent because of the large activation energies for oxide migration and desorption. For example, in simulations at $610\,^{\circ}\mathrm{C}$ J_p is less than half as large as at $590\,^{\circ}\mathrm{C}$. Hence small uncertainties in temperature will have rather large consequences for J_p. Similarly, a relatively small change in the activation energy for oxide migration or desorption will have a significant effect on the cluster number. In addition, the attempt rates for migration and desorption are not known with any precision; an order of magnitude change in one or the other of these will have a corresponding effect on the rate of cluster formation at any given temperature or etching rate.

Another point that addresses the discrepancy between experiment and simulations is that in the simulations we do not allow members of an oxide cluster to dissociate or desorb. One may surmise that a small cluster, consisting of two or three SiO complexes, is not stable. If small clusters dissociate, that will decrease the rate at which larger clusters are produced and hence this effect will also bring the simulations into closer agreement with experiments. Moreover, breakup of small clusters will also affect the dependence of J_p on the oxygen pressure, in particular causing J_p to vary as a larger power of P than P^2, and that is also observed in experiments.[21]

To examine issues related to oxide-island formation in greater detail, we have done extensive simulations of the simplified model described at the end of Sec. II, using systems as large as 1000 cells on a side and depositing as many as 100 layers of oxygen (a "layer" being one oxygen atom per cell) on the surface. Three versions of the model were simulated. In the first (a), a pair of SiO complexes on neighboring sites is inert and cannot be broken; in the second (b), such a pair can be broken via the desorption of a member of the pair, and the probability for a member of a pair to desorb is the same as that for an isolated SiO to desorb; the third version (c) also allows a member of a pair to desorb but the probability is reduced relative to that in (b) by a factor of $\exp(-\epsilon_{ci}/kT)$, which expresses the possible presence of a barrier to the dissociation of the SiO pair. In both (b) and (c), clusters of three or more SiO's are inert.

The qualitative results from the simulations may in cases (a) and (b) be characterized by the statement that the rate of production of stable, or inert, oxide islands can

be reasonably well fit, in the ranges of P and T simulated, by the relation

$$J_p \propto P^a e^{\epsilon/kT}. \tag{4.1}$$

For (a), $a = 1.9 \pm 0.1$ and $\epsilon = 4.04 \pm 0.10$ eV; for (b), $a = 3.0 \pm 0.05$ and $\epsilon = 7.64 \pm 0.10$ eV; for (c), the fit to such a simple function is not good, but there is a range of P and T such that $a = 2.4 \pm 0.1$ and $\epsilon = 7.14 \pm 0.1$ eV produce a fit that is not too bad. We should emphasize, however, that the results fit a single simple exponential function of the inverse temperature and a simple power of P only because of the relatively narrow ranges of P (or τ_l) and T simulated, ranges which are comparable to those studied in the experiments.

The conclusions of the simulations are quite consistent with those from simple rate equations describing the deposition, diffusion, cluster growth, and evaporation processes. The rate equations are

$$\frac{dn_1}{dt} = R - \alpha n_1 + \beta n_2 - 2D\gamma_1 n_1^2 - D\sum_{m=2}^{\infty} \gamma_m n_1 n_m, \tag{4.2}$$

$$\frac{dn_2}{dt} = -\beta n_2 + D\gamma_1 n_1^2 - D\gamma_2 n_1 n_2, \tag{4.3}$$

and

$$\frac{dn_m}{dt} = D\gamma_{m-1} n_1 n_{m-1} - D\gamma_m n_m n_1, \quad m > 2. \tag{4.4}$$

The density of SiO clusters of size m is n_m; R is the rate per unit area at which oxygen atoms (two per molecule) striking the surface are adsorbed, α is the probability per unit time that a monomer desorbs while β is the same for a SiO that is a member of a dimer; D is the diffusion constant for a monomer; and γ_m expresses the probability that a monomer will overcome the extra barrier ϵ_{ci} to join a cluster of size m. Thus $R \propto P$ and the dependence of each of the other parameters in the rate equations on the parameters of the microscopic model is $D \propto \exp(-\epsilon_{cd}/kT)$, $\alpha \propto \exp(-\epsilon_{ce}/kT)$, and $\gamma_m \propto \exp(-\epsilon_{ci}/kT)$. As for β, it is zero for version (a) of the model, proportional to α for (b), and proportional to $\alpha \exp(-\epsilon_{ci}/kT)$ for (c). Note that all γ_m are assumed to have the same temperature dependence. They increase with m because a large cluster presents a large target to a diffusing SiO. Finally, the rate equations are incomplete in that they do not describe the effect of clusters coalescing as they grow and overlap one another. Neither do they incorporate mechanisms by which other possibly important processes may occur, such as dissociation of a SiO dimer without either member desorbing.

The rate R_q at which clusters of size q or larger are formed is found by summing the rates dn_m/dt for all $m \geq q$,

$$R_q = D\gamma_{q-1} n_1 n_{q-1}, \tag{4.5}$$

for $q \geq 3$.

The evolution of the system is roughly as follows: Initially, all n_m are zero. There is at short times a transient behavior and at intermediate times individual n_m's will approach a constant value, the amount of time necessary for this to happen being greater the larger m is. At large times n_1, in particular, decreases because of an increase in the rate at which monomers are absorbed into larger clusters. It is the intermediate regime that we wish particularly to examine. Here, each R_q, for q not too large, approaches a constant. Under this condition, $n_{m-1} = \gamma_{m-2} n_{m-2}/\gamma_{m-1}$, so $R_q = D\gamma_{q-2} n_1 n_{q-2} = R_{q-1}$; that is, all R_q are the same so long as q is small enough that all n_m with $m \leq q$ have become constant. This behavior also appears in the simulations. A typical example is shown in Fig. 5, which displays, for case (b), the number of clusters of size larger than or equal to 3 and the number of size larger than or equal to 7 as functions of the number of layers of oxygen deposited at $T = 600\,^\circ$C and $\tau_l = 250$ sec in a system of size 1000^2 cells. There are fewer of the larger clusters, but after an initial period in which the steady growth rate develops for clusters as large as six SiO's, both growth rates are the same. This behavior persists in the simulations either until clusters begin to merge into one another (an effect not included in the rate equations) or the drain on n_1 produced by the increase in the number of larger clusters becomes appreciable.

By analysis of the rate equations in certain simple limits we obtain results that bear directly on the simulations. First, for all cases simulated by far the majority of the

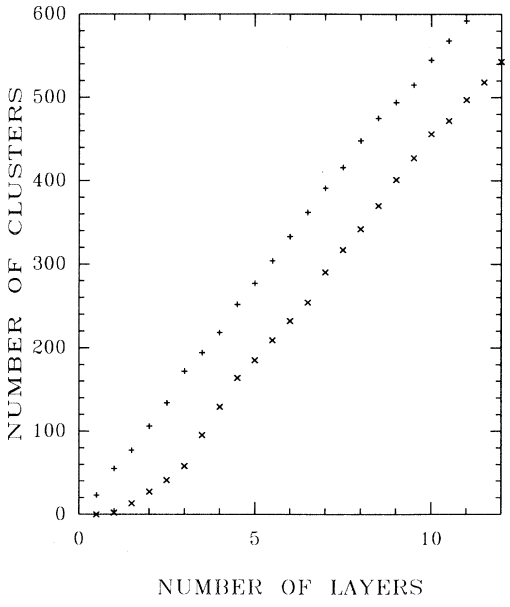

FIG. 5. The cluster number is shown as a function of the number of layers of oxygen adsorbed on the surface for case (b) at 600 °C and $\tau_l = 250$ sec in a system of size 1000^2 cells. The upper (lower) curve gives the number of clusters of size larger than 2 (6).

SiO complexes evaporate from the surface, which means that the equation for n_1 is reasonably approximated by $dn_1/dt = R - \alpha n_1$. Hence, when n_1 saturates, it is

$$n_1 = R/\alpha. \tag{4.6}$$

Similarly, when n_2 settles into a steady state,

$$n_2 = \frac{\gamma_1 D n_1^2}{\beta + D n_1 \gamma_2}. \tag{4.7}$$

These equations and Eq. (4.5) allow us to determine the behavior of R_3. A general analysis is given in the Appendix. For case (a), $\beta = 0$ and $n_2 = \gamma_1 n_1/2\gamma_2$, so that

$$R_3 = \frac{1}{2}\gamma_1 D n_1^2 = \frac{R^2 \gamma_1 D}{2\alpha^2} \propto P^a e^{\epsilon/kT} \tag{4.8}$$

with $a = 2$ and $\epsilon = 2\epsilon_{ce} - \epsilon_{cd} - \epsilon_{ci}$, or $\epsilon = 3.97$ eV using the parameters from the microscopic model. That agrees well with the simulations, which give qualitatively the same behavior with $a = 1.9 \pm 0.1$ and $\epsilon = 4.04 \pm 0.10$ eV.

Version (b) differs from (a) in that β is not zero but is proportional to $\exp(-\epsilon_{ce}/kT)$. The limit $\beta \gg D n_1 \gamma_2$, which means that evaporation of SiO complexes from dimers dominates the addition of a third SiO to a dimer, corresponds to what is observed in simulations of (b). Then $n_2 = \gamma_1 D n_1^2/2\beta$, and

$$R_3 = \frac{D^2 \gamma_2 \gamma_1 R^3}{2\beta\alpha^3} \propto P^a e^{\epsilon/kT}, \tag{4.9}$$

where $a = 3$ and $\epsilon = 4\epsilon_{ce} - 2\epsilon_{ci} - 2\epsilon_{cd}$. The energy in the exponent in this case is 7.94 eV, not hugely different from the value of 7.64 eV extracted from the simulations. Also, the simulations give quite closely $a = 3$.

Finally, for version (c), $\beta \propto \exp[-(\epsilon_{ci} + \epsilon_{ce})/kT]$. If no change is made in the analysis of the rate equations relative to (b) other than this, we will not get the pressure dependence that emerges from the simulations or, for that matter, from the experiments at 600 °C which is more nearly $R_3 \propto P^{2.4}$. However, this behavior can be obtained from the rate equations if the two terms in the denominator on the right-hand side of Eq. (4.7) are comparable in magnitude. The analysis of this case presented in the Appendix produces the curves shown in Figs. 6 and 7. Specifically, Fig. 6 displays $\ln(R_3)$ as a function of $\ln(P/P_0)$ from 590 to 650 °C in steps of 10 °C (the meaning of P_0 is explained in the Appendix); R_3 decreases with increasing T. Any of the curves in the figure is easily interpreted as a straight line. At the highest temperature, the slope of the line approaches 3 which is appropriate in the limit that pairs of SiO clusters are removed predominantly by their being broken rather than by formation of larger clusters. At temperatures somewhat below what is shown, the slope approaches 2. And at temperatures around T_0 (the meaning of T_0 is also explained in the Appendix) there is a region where the slope is around 2.4 or 2.5, as in the experiments and in the simulations of case (c) at 600 °C. The results of the latter, shifted both horizontally and vertically for ease of comparison, are shown in the figure as solid disks.

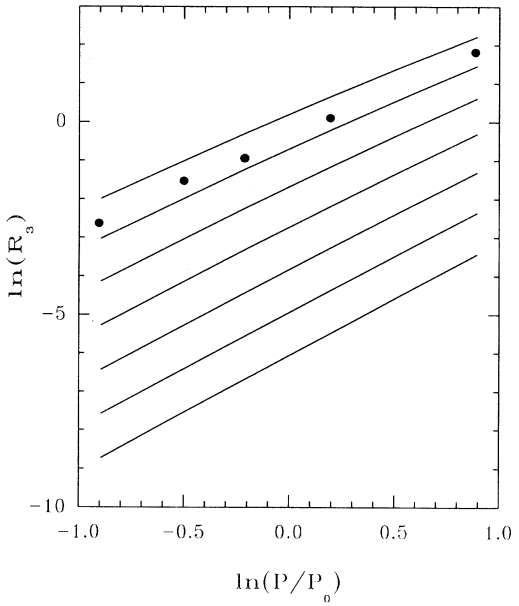

FIG. 6. The logarithm of R_3 as given by Eq. (A7) is shown as a function of $\ln(P/P_0)$ at temperatures from 590 (uppermost curve) to 650 °C (lowest curve). The points are from simulations of case (c) at 600 °C; they have been shifted horizontally and vertically to facilitate comparison with the rate equation predictions.

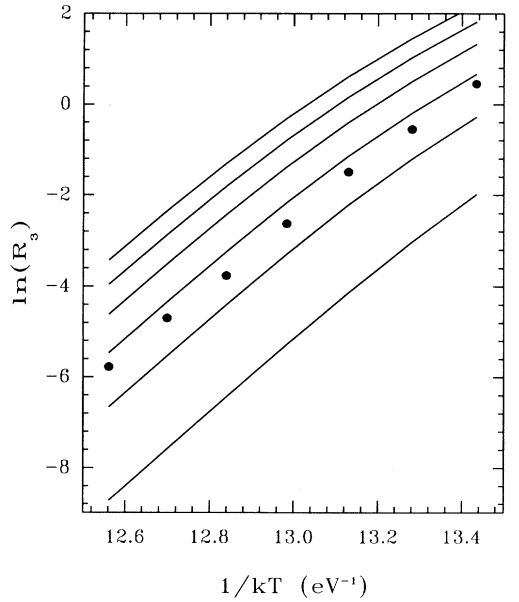

FIG. 7. The logarithm of R_3 as given by Eq. (A7) is shown as a function of $1/kT$ $(\mathrm{eV})^{-1}$ for evenly spaced temperatures between 590 and 650 °C at several pressures around P_0; R_3 increases with P. Results from simulations of case (c) at $\tau_l = 500$ sec are also shown; they have been shifted vertically to facilitate comparison with the curves.

Figure 7 displays the logarithm of R_3 as a function of $1/kT$ at six evenly spaced reduced pressures P/P_0 from $1/\sqrt{6}$ to $6/\sqrt{6}$ and for temperatures between 590 and 650 °C; R_3 increases with P. These curves are distinctly not straight lines, especially at the higher pressures. However, if, as in experiments, one had discrete sets of data with a significant amount of scatter rather than smooth lines, one would very likely be inclined to fit the data with straight lines. The curves of Fig. 7, if approximated by straight lines, have slopes ranging from about 6.4 eV at the highest pressure to 7.8 eV at the lowest pressure. Also shown in the figure as solid disks are the simulation results, shifted by a constant for convenient display, from case (c) at $\tau_l = 500$ sec, corresponding to a pressure of 5×10^{-8} torr if the O_2 sticking coefficient is 0.04. These points show very nearly the same behavior as the lines from the rate equations. If one fits them by a straight line, it has slope of about 7.1 eV.

If experimental determinations[21] of the cluster formation rate at different temperatures are displayed on Arrhenius plots, they suggest an energy ϵ in range of 3.3 – 4.0 eV. The simulations of case (a) are quite close to this value by design; that is, given $\epsilon_{ce} = 3.4$ eV, a value taken from the work of Engstrom *et al.*,[35] the choice of $\epsilon_{cd} + \epsilon_{ci} = 2.84$ eV was made in order that case (a) would lead to a reasonable value of ϵ in comparison with experiments. Our results for cases (b) and (c) make it clear that one must make quite different choices of some parameters if these versions of the model are to achieve acceptable agreement with experiment. On the face of it, ϵ_{cd} and/or ϵ_{ci} would have to be considerably larger, perhaps unreasonably large. The alternative is to make ϵ_{ce} smaller, which would have the additional advantage that one must then decrease significantly ν_{ce} to maintain an appropriate rate of evaporation of SiO's; the value $\nu_{ce} = 4 \times 10^{19}$ sec^{-1} that has been used here is uncommonly high. There is in fact another experimental determination[36] of ϵ_{ce} which is around 3.0 eV; that value, with a lowering of ν_{ce} to around 10^{17} sec^{-1}, would leave the rate of SiO desorption much the same while improving considerably the agreement of the model and experiment as regards the value of ϵ. At this juncture, we are not able to say which strategy is the most appropriate.

Next, we compare the magnitudes of the rates R_q from the simulations with those from experiments. For version (a), as in the simulations of the more complete model taking into account the motions of Si atoms, we find that the rate of production of stable clusters is much larger than in experiments. For (b) the rate from the simulations is significantly less than that from experiments, while for (c), it is again larger than what emerges from experiments. Some specific numbers are the following: The rate of production of oxide islands reported by Seiple and Pelz[21] at 600 °C and 5×10^{-8} torr is about 6×10^7 per sec per cm^2. The corresponding numbers from simulations of versions (a), (b), and (c) of the model are, respectively, 400×10^7, 1.6×10^7, and 120×10^7 per sec per cm^2. The comparison is made assuming the sticking coefficient for an oxygen molecule is 0.04. Similar comparisons are obtained at other temperatures and pressures. The implication is that the model can describe this aspect of the experiments with some quantitative accuracy only by either changing some parameters substantially or allowing breakup of binary SiO clusters.

Another property monitored in the simulations that is relevant to the experimental results is the density of SiO monomers on the portion of the surface that is not covered by oxide. This density remains roughly constant throughout a run as the number and size of oxide clusters increases. It is, of course, larger at lower temperatures and/or higher oxygen pressures. A typical example is version (b) at 640 °C and $\tau_l = 500$ sec, for which the density is $0.000\,30 \pm 0.000\,01$ monomers per cell. Experimentally, a constant etch rate was measured.[22] The constancy of the monomer density in the simulations is consistent with this observation, assuming the etching is in fact due to the evaporation of SiO monomers.

Finally, we address the question of the saturation of the oxide-island density. Experiments in which as many as 1200 L of oxygen strike the surface demonstrate saturation of the oxide-island density. Figure 8(a) shows exper-

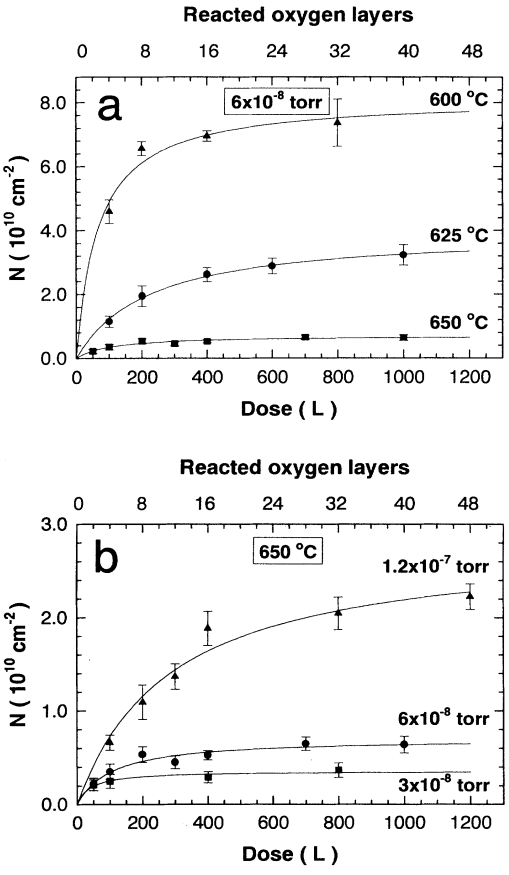

FIG. 8. The cluster number density N is shown as a function of exposure (lower axis) from STM measurements of a 5000^2 Å^2 Si(001) surface at (a) 6×10^{-8} torr and 600, 625, and 650 °C; and (b) 650 °C and 3, 6, and 12.5×10^{-8} torr. The upper axis displays the number of adsorbed layers of oxygen assuming a sticking coefficient of 0.04.

imental measurements of the island density as a function of exposure at $P = 6 \times 10^{-8}$ torr at several temperatures; Fig. 8(b) is the same except at 650 °C and several pressures. The saturation of the island density implies that nucleation of oxide islands is suppressed. It should also be noted, however, that the etch rate (between islands) remains constant.[22]

Long simulations of the simple model were done in an effort to find the saturation of the island density observed in experiments. The results display a maximum in the density; however, the density subsequently decreases as a consequence of the merging or coalescence of growing islands. There are significant differences between the results from experiments and those from simulations. Consider, for example, Fig. 9, which shows simulation results for version (b) that may be directly compared to the experimental results in Fig. 8. Figure 9(a) presents the density of oxide islands as a function of the number of layers of oxygen atoms that stick to the surface (most of which subsequently desorb) for $\tau_l = 250$ sec at 600 and 620 °C. If the sticking coefficient is 0.04, this case corresponds to a pressure of 5×10^{-8} torr and the relation between the abscissas in the figures is that a dose of 100 L corresponds to having four reacted oxygen layers added to the surface. Figure 9(b) is for a temperature of 620 °C and $\tau_l = 250$ and 500 sec.

As stated earlier, simulations of version (b) initially produce oxide clusters at a rate somewhat less than observed in experiments under the same conditions. However, the number of clusters continues to increase for a relatively longer time in the simulations before reaching a maximum, resulting in too many clusters in comparison with the experiments. This particular discrepancy can be fairly easily remedied with small changes in some parameters in the model. A more significant difference between experiments and the model, we believe, is revealed by the fact that the former produces cluster numbers that saturate at the maximum for as long as the experiments have been pursued. The model, on the other hand, produces cluster numbers that reach a maximum and fairly soon thereafter decrease, largely through the coalescence of nearby oxide clusters that grow into each other. This behavior is found in all simulations we have done to date, and we think it unlikely that the discrepancy can be removed by simple adjustment of parameters. Rather, what appears to be needed is a mechanism that would inhibit the nucleation and growth of clusters after a certain number have been formed while maintaining constant the number of SiO monomers which can desorb so that a constant etch rate will be maintained. That would have the twin advantages of preventing too many clusters from forming and of preventing those that are present from merging. We have begun studies of appropriate extensions of the model; some results are presented elsewhere.[23]

A related property is the coverage of the surface by stable oxide islands at various points during the process and in particular when the number of islands approaches a maximum (or saturation, in the case of the experiments). From the simulations we find that the coverage at the maximum cluster density is larger at lower temperatures and larger oxygen pressures, other parameters being equal. For example, at 620 °C and $\tau_l = 250$ sec, and case (b), the coverage is some 5% at the maximum, and it increases to close to 12% at 600 °C and the same τ_l. At these temperatures and half as large a pressure (or twice as large a τ_l), the coverage at the maximum is about two-thirds as large. Experimentally, we estimate an upper limit[37] to the lateral coverage of the oxide clusters at the onset of saturation to be only about 1%.

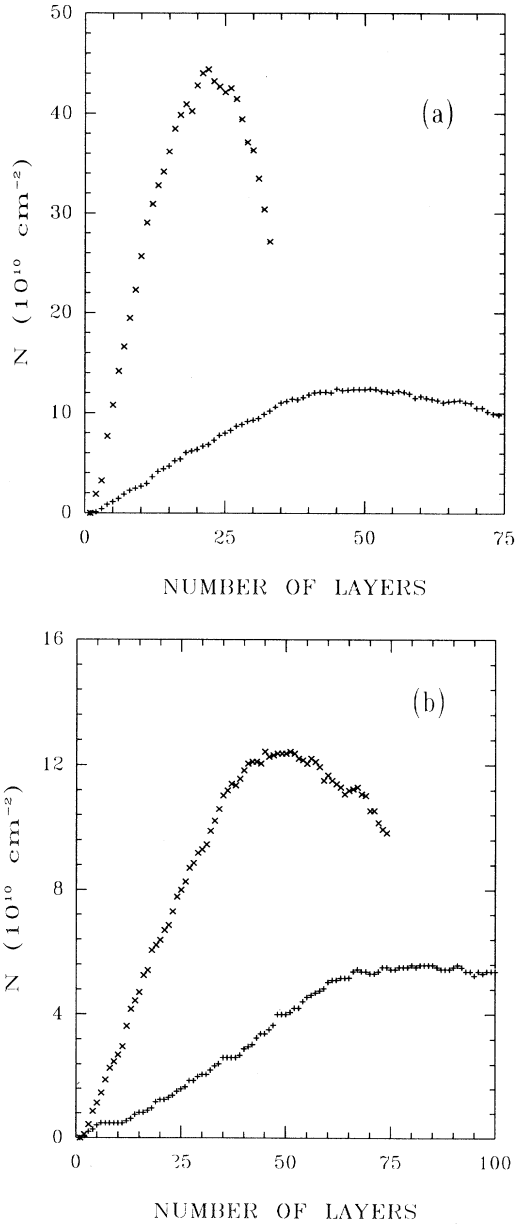

FIG. 9. The cluster number density N as a function of the number of layers of adsorbed oxygen from simulations of case (b) for a 1000^2-cell system at (a) $\tau_l = 250$ sec and 600 (×) or 620 °C (+); and (b) 620 °C and $\tau_l = 250$ (×) or 500 sec (+).

V. SUMMARY

We have presented results from simulations of a lattice model for the evolution of Si(001) surfaces reacting with gaseous molecular oxygen. No attempt has been made to adjust the many parameters in the model so as to obtain detailed quantitative agreement with any particular set of experiments. Rather, the main aim of the work has been to demonstrate that qualitative agreement of many properties with experiment is achieved with a single set of reasonable parameters; further adjustment of parameters would certainly result in improved agreement of some properties with experiment, but we have not so far invested much effort along these lines. The model takes into account the motions of both individual Si atoms and SiO complexes, which it seems reasonable to assume are present on the surface during oxidation. A simpler model, which describes only the diffusion, clustering, and desorption of SiO complexes, has also been simulated extensively with the aim of studying the production and growth of oxide islands over long enough periods of time that saturation of the island number can be observed. These simulations have been compared with our hitherto unreported experimental studies of etching and oxide formation at temperatures in the vicinity of 650 °C.

Although not discussed in detail here, the models reproduce qualitatively a number of known properties of the Si(001) surface without the presence of oxygen. For example, under conditions of epitaxy, B terraces grow with S_B edges becoming much rougher than S_A edges. Long islands of adatoms, predominantly an odd number of dimers in length and a single surface dimer in width, grow in directions perpendicular to the dimer rows on the underlying terrace. Depletion zones with few or no such islands are found on B terraces close to S_B steps, with the zones being larger at higher temperatures. Under conditions of ion sputtering, the B terraces are preferentially retracted with S_B steps showing much greater roughness than S_A steps. Moreover, the dimer rows in the B terrace at the S_B step tend to retract in units of two dimers.

Under conditions that the Si(001) surface is subjected to gaseous molecular oxygen, the version of the model that includes the motions of the Si atoms demonstrates both etching of the Si and the buildup of oxygen clusters, which act as pinning centers for the underlying Si. As a terrace is eaten away, a pinning center prevents etching in its immediate vicinity and so anchors a relatively long "finger" as material on the terrace on the two sides of the pinning center is removed. Eventually, the finger is eaten through from the sides, leaving an outcropping capped by an oxide cluster, the outcropping growing ever higher as material around it continues to be removed. The dependence of the rate at which oxide clusters are formed has been studied as a function of temperature and oxygen pressure and is similar to what emerges from the experiments at low doses. Additional simulations of a simplified model that does not include the motions of the Si atoms were done to examine oxide-cluster nucleation and growth at extended doses.

The general conclusion of our studies is that these models can be made to agree closely with many measured properties of the Si(001) surface. However, one important property of the silicon-oxygen system that seems beyond the present models is the saturation of the number of oxide clusters observed after long exposure. All versions of the model lead to a maximum in the cluster number followed soon after by a sharp decrease as clusters coalesce. We are currently considering a model originally proposed by Engstrom and co-workers in Ref. 35 that involves two distinct oxygen bonding configurations. Preliminary rate equation analysis and Monte Carlo simulations show qualitative agreement with the saturation observed at extended doses.[23]

ACKNOWLEDGMENTS

This work was supported in part by NSF Grants Nos. DMR-9406936 and DMR-9357534. The simulations were done using the OSU Department of Physics VAXcluster.

APPENDIX: RATE EQUATION ANALYSIS

Equations (4.5) through (4.7) combine to give

$$R_3 = \frac{\gamma_1\gamma_2 D^2 R^3/\alpha^3\beta}{1 + DR\gamma_2/\alpha\beta}. \tag{A1}$$

We display all of the temperature dependence in this expression explicitly by writing $\gamma_1 = \gamma_{10}\exp(-\epsilon_{ci}/kT)$, and similarly for γ_2, D, α, and β. Also, the pressure dependence is displayed by writing $R = R_0 P$. With these substitutions we have

$$R_3 = \frac{C_1 P^3 e^{(4\epsilon_{ce}-2\epsilon_{cd}-\epsilon_{ci})/kT}}{1 + C_2 P e^{(2\epsilon_{ce}-\epsilon_{cd})/kT}}, \tag{A2}$$

where C_1 and C_2 are constant parameters composed of γ_{10}, R_0, etc.,

$$C_1 = \frac{\gamma_{10}\gamma_{20} D_0^2 R_0^3}{\alpha_0^3\beta_0} \tag{A3}$$

and

$$C_2 = \frac{D_0 R_0 \gamma_{20}}{\alpha_0\beta_0}. \tag{A4}$$

Case (a), for which SiO dimers do not dissociate, corresponds to the limit $\beta_0 \to 0$. The opposite limit, which turns out to be essentially case (b) of the simulations, is such that the second term in the denominator of Eq. (A2) is negligible in comparison with the first term.

To analyze the intermediate regime, where the terms in the denominator are comparable, we rewrite C_1 and C_2 in terms of two equivalent parameters, called P_0 and T_0 (because they have dimensions of pressure and temperature), which are defined in terms of C_1 and C_2 by

$$C_1 \equiv \frac{e^{-(4\epsilon_{ce}-2\epsilon_{cd}-\epsilon_{ci})/kT_0}}{P_0^3} \tag{A5}$$

and

$$C_2 \equiv \frac{e^{-(2\epsilon_{ce}-\epsilon_{cd})/kT_0}}{P_0}. \tag{A6}$$

In terms of P_0 and T_0, R_3 can be written as

$$R_3 = \frac{e^{(4\epsilon_{ce}-2\epsilon_{cd}-\epsilon_{ci})(1/kT-1/kT_0)}(P/P_0)^3}{1+e^{(2\epsilon_{ce}-\epsilon_{cd})(1/kT-1/kT_0)}(P/P_0)}. \tag{A7}$$

The regime of interest is the one where the two terms in the denominator are comparable. They are comparable in particular for $P \approx P_0$ and $T \approx T_0$. Figures 6 and 7 show the behavior of R_3 as functions of P and T in appropriate ranges. Specifically, P/P_0 varies from $1/\sqrt{6}$ to $6/\sqrt{6}$ while T_0 is set equal to 600 °C and T ranges from 590 to 650 °C.

[1] T. Sakamoto, N. J. Kawai, T. Nakagawa, K. Ohta, and T. Kojima, Appl. Phys. Lett. **47**, 617 (1985).

[2] R. Hamers, U. K. Köhler, and J. E. Demuth, Ultramicrosc. **31**, 10 (1989); J. Vac. Sci. Technol. A **8**, 195 (1990).

[3] M. G. Lagally, R. Kariotis, B. S. Swartzentruber, and Y.-W. Mo, Ultramicrosc. **31**, 87 (1989).

[4] M. G. Lagally, Y.-W. Mo, R. Kariotis, B. S. Swartzentruber, and M. B. Webb, in *Kinetics of Ordering and Growth at Surfaces*, edited by M. G. Lagally (Plenum, New York, 1990).

[5] A. J. Hoeven, D. Dijkkamp, E. J. van Loenen, J. M. Lenssinck, and J. Dieleman, J. Vac. Sci. Technol. A **8**, 207 (1990).

[6] A. J. Hoeven, J. M. Lenssinck, D. Dijkkamp, E. J. van Loenen, and J. Dieleman, Phys. Rev. Lett. **63**, 1830 (1989).

[7] Y.-W. Mo and M. G. Lagally, Surf. Sci. **248**, 313 (1991).

[8] P. Bedrossian and T. Klitsner, Phys. Rev. Lett. **68**, 646 (1992).

[9] P. Bedrossian, Surf. Sci. **301**, 223 (1994).

[10] H. Feil, H. Zandvliet, M. Tsai, J. Dow, and I. S. T. Tsong, Phys. Rev. Lett. **69**, 3076 (1992); H. Zandvliet *et al.*, Phys. Rev. B **46**, 7581 (1992).

[11] P. Bedrossian, J. Houston, J. Tsao, E. Chason, and S. T. Picraux, Phys. Rev. Lett. **67**, 124 (1991).

[12] P. Bedrossian and T. Klitsner, Phys. Rev. B **44**, 13 783 (1991).

[13] J. J. Lander and J. Morrison, J. Appl. Phys. **33**, 2089 (1962).

[14] F. W. Smith and G. Ghidini, J. Electrochem. Soc. **129**, 1300 (1982).

[15] Y. Ono, M. Tabe, and H. Kageshima, Phys. Rev. B **48**, 14 291 (1993).

[16] M. Udagawa, M. Niwa, and I. Sumita, Jpn. J. Appl. Phys. **32**, 282 (1993).

[17] K. E. Johnson and T. Engel, Phys. Rev. Lett. **69**, 339 (1992).

[18] A. Feltz, U. Memmert, and R. J. Behm, Chem. Phys. Lett. **192**, 271 (1992).

[19] J. Seiple, J. Pecquet, Z. Meng, and J. P. Pelz, J. Vac. Sci. Technol. A **11**, 1649 (1993).

[20] F. Donig, A. Feltz, M. Kulakov, H. E. Hessel, U. Memmert, and R. J. Behm, J. Vac. Sci. Technol. B **11**, 1955 (1993).

[21] J. V. Seiple and J. P. Pelz, Phys. Rev. Lett. **73**, 999 (1994).

[22] J. V. Seiple and J. P. Pelz, J. Vac. Sci. Technol. A **13**, 772 (1995).

[23] J. V. Seiple, C. Ebner, and J. P. Pelz (unpublished).

[24] K. C. Pandey, in *Proceedings of the 17th International Conference on the Physics of Semiconductors, San Francisco, California, 1984*, edited by D. J. Chadi and W. A. Harrison (Springer, New York, 1985).

[25] R. Biswas and D. R. Hamann, in *Computer-Based Microscopic Description of the Structure and Properties of Materials*, edited by J. Broughton and W. Krakow, MRS Symposia Proceedings No. 63 (Materials Research Society, Pittsburgh, 1995), p. 173.

[26] F. F. Abraham and I. P. Batra, Surf. Sci. **163**, L752 (1985).

[27] T. A. Weber, in *Computer-Based Microscopic Description of the Structure and Properties of Materials* (Ref. 25).

[28] S. A. Barnett and A. Rockett, Surf. Sci. **198**, 133 (1988).

[29] A. Rockett, Surf. Sci. **227**, 208 (1990).

[30] H. B. Elswijk, A. J. Hoeven, E. J. van Loenen, and D. Dijkkamp, J. Vac. Sci. Technol. **9**, 451 (1991).

[31] E. Chason and B. W. Dodson, J. Vac. Sci. Technol. **9**, 1545 (1991).

[32] V. M. Bedanov and D. N. Mukhin, Surf. Sci. **278**, 364 (1992).

[33] H. J. W. Zandvliet, H. B. Elswijk, and E. J. van Loenen, Surf. Sci. **272**, 264 (1992).

[34] N. Kitamura, B. S. Swartzentruber, M. G. Lagally, and M. B. Webb, Phys. Rev. B **48**, 5704 (1993).

[35] J. R. Engstrom, D. J. Bonser, M. M. Nelson, and T. Engel, Surf. Sci. **256**, 317 (1991).

[36] M. L. Yu and B. N. Eldridge, Phys. Rev. Lett. **58**, 1691 (1987).

[37] The coverage is a difficult quantity to obtain experimentally because the spatial extent of the oxide may be much smaller than the area of the Si island that it pins. In addition, a blunt tip can cause islands to appear laterally larger than they may actually be. Another uncertainty is the extent to which oxygen may react and exchange with subsurface layers.